36 Variations in Exhaust Emissions and Combustion Stability with Control Parameters during Idle Operations of an SI Engine

(1)Duk-Sang Kim, (1)Yong-Seok Cho, (2)Chang Gi Kim and (2)Kern Yong Kang
(1)Graduate School of Automotive Engineering, Kookmin University, (2)Korea Institute of Machinery and Materials
(1)861-1, Jeongneung-dong, Songbuk-gu, Seoul 136-702, Korea, (2)171, Jang-dong, Yuseong-gu, Daejon 305-343, Korea

Rapid warm up of catalyst and improved combustion stability are crucial factors for reduction of harmful exhaust emissions during cold start of an SI engine. Previous studies showed that retarded ignition timing and reduced valve overlap produced higher exhaust gas temperatures resulting in faster light-off of catalysts. This study focuses on analysis of exhaust emissions with changes of ignition and exhaust valve timings during idle operations. Pressure variations in the combustion chamber are also measured and analyzed to investigate combustion stability. A combustion analyzer, designed for this study, converts pressure data to combustion characteristics such as imep and COV. These data provide better understandings of combustion with engine control parameters. Changing effects of exhaust valve timing on residual gas fraction are also investigated using transient CFD analysis. Experimental results and numerical analysis show that proper advance of exhaust valve timing is effective to improve COV and CO emissions due to a decrease in mass fraction of residual gas. HC emissions are closely related to ignition timing. Both ignition and exhaust valve timings influence NOx emissions. It is expected that optimal control of ignition and exhaust valve timings in the cold start period and idle operation will reduce harmful exhaust emissions and improve combustion stability of the engine

Keywords **: Idle operation, Ignition timing, Exhaust valve timing, Exhaust emission, Combustion stability**

1. INTRODUCTION

Three-way catalyst (TWC), the successful application of exhaust gas after-treatment to SI engines, is very effective to lower the emission levels from gasoline-engine powered vehicles. The conversion rates of CO, HC and NOx of a TWC are above 90%, after it is fully activated. However, it also has inherent problems related to catalytic chemical reactions. Since the catalyst stays at lower temperatures during cold start period of a vehicle, harmful species such as CO and HC pass through the TWC without catalytic reaction and the levels of exhaust emissions are very high in this period. Therefore, the key technologies to meet the stringent emission regulations such as LEV, ULEV and SULEV of CARB, and to protect the air quality in urban areas are closely related to reduce the time required for heating a catalyst to the light-off temperature in the cold start period [1][2].

Previous studies showed that changes in spark ignition timing significantly affect exhaust gas temperature in cold start period [3][4]. When spark ignition timing is retarded, the start of combustion is delayed, resulting in a lower maximum cylinder pressure. On the other hand, flame stays up to a later stage of the expansion stroke and the exhaust gas temperature is higher than that of the normal spark ignition. Although energy loss is considerable with retarded ignition timing, rapid warm-up of catalyst in a cold start period can be achieved from an increase in the exhaust gas temperature. Recent development in engine control unit (ECU) and variable valve timing (VVT) technology is also very helpful to minimize the warm-up time of catalysts in cold start. A VVT system can change the intake or exhaust valve timings to optimize the gas exchange processes, and the engine operating parameters such as engine speed, load and coolant temperature change[5]. Changes in the intake and exhaust valve timings affect flame speed and temperature. A proper change in valve timing can also raise exhaust gas temperature for rapid warm-up of the catalysts in the cold start period. Such changes in spark and valve timings can affect combustion stability that leads to poor idle quality and exhaust emissions. Consequently, proper changes in these timings should result in higher exhaust temperatures while maintaining or improving combustion stability and exhaust emissions.

The main objectives of this study are to find out the effects of the spark ignition timing and exhaust valve timing on combustion stability and exhaust gas compositions. Another goal of this study is to analyze changes in the mass fraction of residual gas with respect to changes in exhaust valve timings. At first, the effects of exhaust valve timing and spark ignition timing on idle operation were investigated through engine bench tests. A variable timing camshaft, fabricated for this study, was used to change the exhaust valve timings. A programmable ECU was used to change the spark ignition timings. Combustion characteristics and exhaust gas compositions were measured and analyzed under various ignition and exhaust valve timing conditions. Variations in combustion stability under these test conditions were also investigated. Finally, the effects of exhaust valve timings on residual gas fractions in the cylinder were analyzed using a CFD code.

2. EXPERIMENTAL SETUP

2.1. Measurements

A 2-liter, naturally aspirated, four-cylinder SI engine is used as a test engine. Table 1 describes specifications of the engine. Fig. 1 shows a schematic diagram of the experimental setup. A piezoelectric pressure transducer (Kistler, 6052B) measures pressure changes of cylinder #1 in which a spark-plug type mount is installed. Pressure measurements are synchronized with the signals from a crank angle encoder that generates pulses at every 0.1 degree of crank angle. Therefore, 7200 pressure data are acquired in one cycle of cylinder #1 and the number of data is sufficient to evaluate cyclic variations through indicated diagrams [6]. The charge signals for pressure are converted to voltage signals by a charge-to-voltage amplifier, and the voltage signals are measured and analyzed by a data acquisition system (National Instruments, DAQCard-MIO-16E4 and BNC-2090). An absolute pressure sensor (Kistler, 4045B) measures pressure in the intake plenum chamber, and calibrates the drift of the pressure transducer. The data acquisition system also measures signals from TDC sensor of the engine in the same manner, and determines where the top center is located on pressure curves.

Table 1 Specifications of test engine.

Items	Specifications
Type	4 cylinder, spark-ignition, In-line, DOHC
Bore	82 mm
Stroke	93.5 mm
Compression ratio	10.1
Idle speed	700±100 rpm
Spark timing on idle	BTDC 8° ±5°
Intake valve timing	BTDC 9°/ABDC 43°
Exhaust valve timing	BBDC 50°/ATDC 6°
Valve overlap	15°

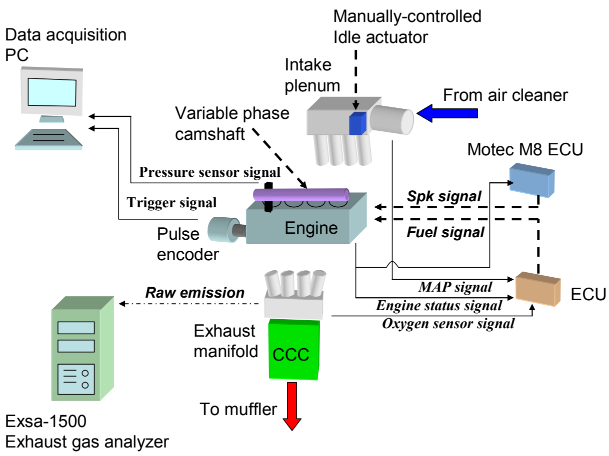

Fig. 1 Schematic diagram of experimental setup

The measured pressure data are used to determine the coefficient of variation in imep (COV_{imep}) which is an index of combustion stability. A PC-based combustion analyzer using LabVIEW collects the data and calculates COVs. At first, in order to obtain p-Θ diagrams from the voltage signals, the analyzer calculates absolute cylinder pressure from the voltage signals, intake pressure signals and scale factor of the amplifier. After that, the analyzer calculates cylinder volume from synchronized crank angles in each cycle to obtain P-V diagrams. Engine specifications and measurement conditions must be supplied for consequent calculations. Numerical cyclic integrations are carried out from P-V curves to find out the imep values of each cycle. These imep values are used to calculate the COV_{imep} by equation (1).

$$COV_{imep} = \frac{\sigma_{imep}}{imep} \times 100(\%) \qquad (1)$$

An exhaust gas analyzer (Horiba, EXSA-1500) is used to measure exhaust gas compositions. It measures the concentrations of CO, HC and NOx as well as the air-fuel ratio. Changes in engine control parameters lead to the changes in exhaust gas compositions, but the effects are smaller after exhaust gas passes through the catalyst. Therefore, as explained in the Fig. 1, a sampling probe is installed at the end of exhaust manifold to measure the engine-out emissions.

2.2. Controls of valve and ignition timings

In the test engine, a variable timing camshaft that can change the phase of cam events is installed for the control of exhaust valve timings. Fig. 2 shows a variable timing camshaft mounted on the test engine and a modified sprocket for the experiments. The cam sprocket and chain pulley can be disassembled from the camshaft while the engine is on the test bench. Exhaust cam phase can be changed by simply turning the camshaft when the sprocket and pulley are disconnected. As shown in Fig. 2, there are 16 keyholes on the pulley and 15 holes on the camshaft mount. Consequently, the minimum change of cam phase is 1.5° in cam angle and 3° in crank angle.

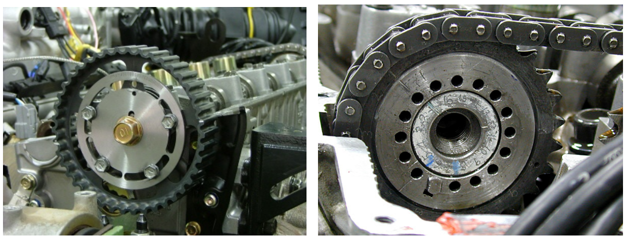

Fig. 2 Variable timing camshaft mounted on test engine

Generally, exhaust gas compositions are very sensitive with the changes of air-fuel ratio. In a conventional engine, engine management system (EMS) controls various parts of the engine such as an idle speed actuator (ISA), fuel injectors and an ignition system. In this study, we needed to handle only the ignition system without changing other conditions that may affect air-fuel ratio. Furthermore, the change in ignition timing leads to variations of engine torque. Under the idle condition, engine speed is very sensitive to changes in ignition timing.

At first, the original ECU (ECU #1) communicates with every sensors and actuators of the engine and a programmable ECU (Motec M8; ECU #2) receives data from a crank angle sensor and a TDC sensor that are crucial to determine and control ignition timing. The ECU #2 supplies spark signals to the ignition system. At the same time, spark signals from ECU #1 are supplied to a dummy ignition system, in order to prevent malfunctions of the OBD system. Ignition timings of ECU #2 are determined by a control PC. In this way, it is possible to control the ignition system as an open-loop circuit, while maintaining other parameters controlled by ECU #1. However, the ISA is still under control of ECU #1 and there is no way for ECU #1 to realize such changes in ignition timings. Even though ECU #1 accurately controls the ignition system, the engine does not run at the same operating conditions that it is programmed. In preliminary tests, a problem associated with open-loop control of ignition timing was found. ECU #1 controls the ISA in an unstable manner, while it is trying to maintain stability of the engine. To solve the problem, a manually-controlled idle actuator with a small valve was used instead of the ISA. The valve is wide open when the engine is in cranking period, and the degree of valve opening is controlled manually to run the engine at the same engine speed in every test condition.

2.3. Test conditions

In this study, measurements are performed after coolant temperature of the engine becomes over 82.5℃ that is a criterion of steady-state operation. The timings of exhaust valve open (EVO) are BBDC 50° CA for the baseline case, BBDC 53°, 56°, 59° and 62° CA for the advanced cases, and BBDC 47°, 44°, 41° and 38° CA for the retarded cases. Crank angles increase when the timings are advanced and decrease when they are retarded. Therefore, the differences in crank angles are indicated as positive when advanced, and as negative when retarded. At each condition of EVO, ignition timings are changed from BTDC 15° to ATDC 3° at an interval of 3° CA. The idle valve is controlled to maintain the engine speed at 900 rpm under each test condition, and the range of actual engine speed was 900±30 rpm. Cylinder pressure curves of 30 consecutive cycles are captured for one measurement, and it is repeated ten times. In the same way, exhaust gas measurements are also repeated ten times and the representative values shown in the paper are averages of the measurements.

3. NUMERICAL ANALYSIS

The air motion can be described by the principle of the conservation of mass and momentum. In order to analyze the characteristics of turbulent airflow motion, a time-averaged Reynolds equation and turbulence model are applied. In addition, turbulent diffusion model should be considered to analyze the mixing of fresh-air and burned gas that occupies the cylinder at the end of exhaust stroke. In this study, the commercial software FLUENT is used to perform the transient analysis of airflow motion and diffusion. The governing equations applied to FLUENT [7] are summarized as follows.

- Continuity equation

$$\frac{\partial(\rho U_i)}{\partial x_i} = 0 \tag{2}$$

- Reynolds equation with turbulent momentum

$$\frac{\partial(\rho U_i)}{\partial t} + U_j \frac{\partial(\rho U_i)}{\partial x_j} = -\frac{\partial P}{\partial x_i} + \frac{\partial}{\partial x_j}\left(\mu \frac{\partial U_i}{\partial x_j} - \overline{\rho u_i u_j}\right) \tag{3}$$

- Boussinesq model

$$\overline{\rho u_i u_j} = \mu_t\left(\frac{\partial U_i}{\partial x_j} + \frac{\partial U_j}{\partial x_i}\right) - \frac{2}{3}\rho k \delta_{ij}, \quad \mu_t = \frac{C_\mu \rho k^2}{\varepsilon} \tag{3}$$

- Transport equation of standard $k-\varepsilon$ model

$$\frac{\partial(\rho k)}{\partial t} + \frac{\partial(\rho U_i k)}{\partial x_i} = \rho P - \rho\varepsilon + \frac{\partial}{\partial x_i}\left[\left(\mu + \frac{\mu_t}{\sigma_k}\right)\frac{\partial k}{\partial x_i}\right] \tag{4}$$

$$\frac{\partial(\rho\varepsilon)}{\partial t} + \frac{\partial(\rho U_i \varepsilon)}{\partial x_i} = C_{\varepsilon_1}\frac{\rho P \varepsilon}{k} - C_{\varepsilon_2}\frac{\rho\varepsilon^2}{k} + \frac{\partial}{\partial x_i}\left(\left(\mu + \frac{\mu_t}{\sigma_\varepsilon}\right)\frac{\partial \varepsilon}{\partial x_i}\right) \tag{5}$$

- Production term P in the equation (4) and (5)

$$P = \frac{\mu_t}{\rho}\left(\frac{\partial U_i}{\partial x_j} + \frac{\partial U_j}{\partial x_i} - \frac{2}{3}\frac{\partial U_m}{\partial x_m}\delta_{ij}\right)\frac{\partial U_i}{\partial x_j} - \frac{2}{3}k\frac{\partial U_m}{\partial x_m} \tag{6}$$

- Boundary conditions for standard $k-\varepsilon$ model;

$$k = 1.5(I \times U)^2, \ \varepsilon = \frac{C_\mu^{0.75} k^{1.5}}{L} \tag{7}$$

Notation I is the turbulence intensity, Cμ stands for the turbulence coefficient, and L is the characteristic length.

Each coefficient is determined by general values of in-pipe flow as such.

$$C_\mu = 0.09, C_{\varepsilon_1} = 1.44, C_{\varepsilon_2} = 1.92, \sigma_k = 1.0, \sigma_\varepsilon = 1.3 \tag{8}$$

- Turbulent mass diffusion model

$$\frac{\partial(\rho Y_i)}{\partial t} + \frac{\partial(\rho U_j Y_i)}{\partial x_j} = -\frac{\partial J_{ij}}{\partial x_i} + S_i, \ J_{ij} = -\left(\rho D_i + \frac{\mu_t}{Sc_t}\right)\frac{\partial Y_i}{\partial x_j} \tag{9}$$

Notation D_i means diffusion coefficient of species i, and Sc_t is turbulent Schmidt number.

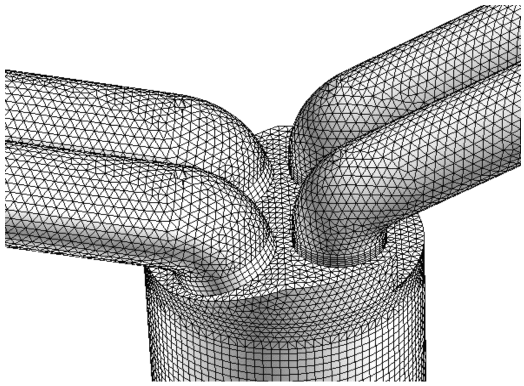

Fig. 3 Mesh generation of the cylinder, intake and exhaust ports

Table 2 Boundary condition of numerical analysis

Item	Specification
Engine idle speed	700rpm
Baseline IVO / IVC	BTDC 9˚CA / ABDC 43˚CA
Baseline EVO / EVC	BBDC 50˚CA / ATDC 6˚CA
Changes of EVO	12˚CA advanced and retarded
Property of residual gas	Nitrogen
Intake pressure	40 kPa
Exhaust pressure	100 kPa
Turbulence model	Standard k-ε model
Initial turbulence kinetic energy	2% of inlet velocity
Initial turbulence characteristic length	30mm

Fig. 3 indicates 3-dimensional simulation model of the cylinder, intake and exhaust ports. The design of grids is crucial to improve the accuracy of a CFD analysis. However, the shape of cylinder head, including intake and exhaust system, is very complex, and if the amount of cells is increased in order to cover grids to such complex geometry, CPU time drastically increases for the CFD code to solve the problems. Automatic grid generation technique is very useful to improve quality of grid without excessive increase in number of cells. In this study, GAMBIT, an automatic grid generator for FLUENT, generates the mesh into the CAD model of the cylinder. Furthermore, in particular regions where piston or valve motion should be considered, hexagonal grids are assigned to apply re-mesh and layer methods of FLUENT. The re-mesh and layer methods enable increase or decrease of the number of cells according to the change of time. Other regions that have no change of geometry with respect to time have tetrahedral grids. Average number of cells is about 300,000. It costs about 35 hours to solve turbulent flow and diffusion during exhaust and intake processes divided into 1500 steps of time in a Pentium 2.4 GHz PC. The boundary and initial conditions of the analysis are summarized in Table 2. During intake stroke in an idle or a cold-start operation, pressure of the intake port becomes very low, due to the small open area of the throttle valve and idle actuator. In all preliminary tests, intake pressure was set at 40 kPa absolute pressure.

4. RESULTS AND DISCUSSION

4.1. Combustion stability

Fig. 3 shows distribution of COV_{imep} with respect to changes in ignition and EVO timings. It is clear that the COV_{imep} strongly depends on changes in EVO, rather than changes in ignition timings. A main reason to explain the phenomena is changes in valve overlap period. When using the variable timing camshaft, it is possible to change the exhaust valve open and close timings but there is no way to change the cam profile. It means when the valve open timing is retarded or advanced, the valve close timing should be changed accordingly. Only the exhaust valve timing is changed in this experiment, and the intake/exhaust valve overlap period should be altered because there is no change in intake valve timing. During idle operation of an SI engine, pressure in the intake manifold is much lower than that in the exhaust manifold. This causes a backward flow of exhaust gas during valve overlap period and increases the amount of residual gas in the next cycle. When the exhaust valve timing is advanced, the overlap becomes shorter. On the contrary, when the exhaust valve timing is retarded, the overlap becomes longer. Therefore, a retarded EVO lead to a longer duration of valve overlap and increase the amount of residual gas, resulting in a lower flame speed and poor engine stability especially in idle conditions. Fig. 3 also shows that the changes in ignition timings have no strong influences on variations of COV_{imep}. Small changes in COV_{imep} due to ignition timings occur when EVO is extremely retarded or advanced.

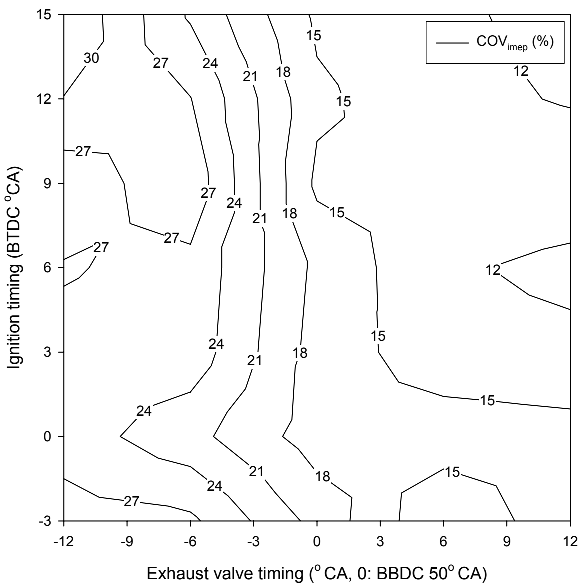

Fig. 4 Distribution of COV_{imep} with respect to ignition and EVO timings

Numerical analysis also shows these changes in burned mass fraction of the cylinder with respect to EVO timings. Fig. 5 shows distributions of residual gas fraction with various EVO timings at ATDC 10° CA. Blue colored region indicates that the region is filled with fresh air and red indicates burned gas in the cylinder. From IVO to TDC, burned gas of the cylinder flows backward to intake ports, due to the lower intake pressure. When the EVO timing is retarded, it is clearly shown that the amount of backward flow is much higher compared with other EVO timings. Fig. 6 also shows distributions of residual gas fraction at ATDC 150° CA when the cylinder undergoes intake process. Backward flow of residual gas enters the cylinder during intake process, and the gas mixes with the fresh air. Consequently, the residual gas fraction of the cylinder becomes higher when the EVO timing is retarded. Through the analysis, it is clearly understood that the stability of combustion is dominant on EVO timings, due to the changes in the residual gas fraction.

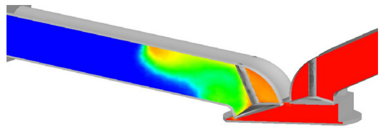

(a) Advanced EVO (Valve overlap : 3° CA)

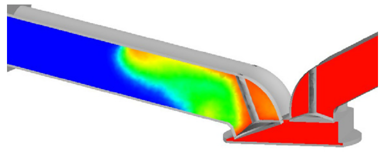

(b) Baseline EVO (Valve overlap : 15° CA)

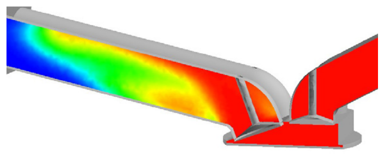

(c) Retarded EVO (Valve overlap : 27° CA)

Fig. 5 Numerical analysis of residual gas fraction with respect to EVO timings at ATDC 10° CA

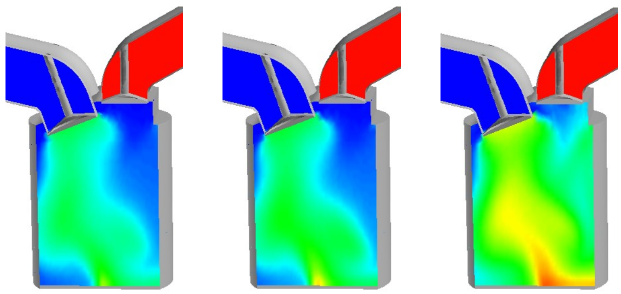

(a) Advanced EVO (b) Baseline EVO (c) Retarded EVO

Fig. 6 Numerical analysis of residual gas fraction with respect to EVO timings at ATDC 150° CA

Fig. 7 indicates quantitative residual mass fraction of the cylinder with respect to EVO timings. Before IVO (BTDC 9° CA), there exists no fresh air in the cylinder and the residual gas fraction is unity. After IVO to EVC, backward flow of residual gas into the intake port occurs, and the residual gas fraction is still unity even though the intake valve is open. After EVC, fresh air is supplied to the cylinder and the residual gas fraction becomes lower. In the case of retarded EVO, residual gas fraction is very high compared with other cases due to the increased amount of backward flow.

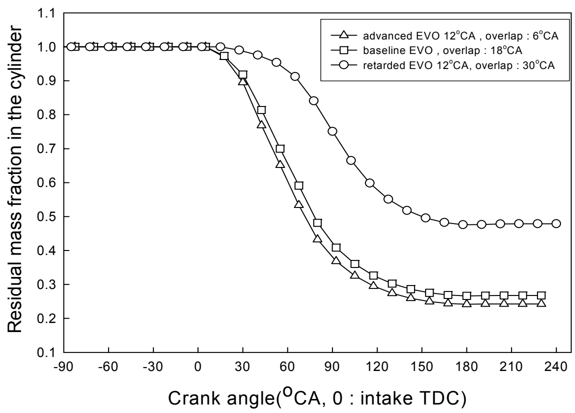

Fig. 7 Residual mass fraction in the cylinder with changes of EVO timings

4.2. Emission level

Emission concentration of CO is very sensitive to the amount of fresh air, and the changes in residual gas fraction would result in the variations of CO emissions. Fig. 8 indicates the CO emission distribution with ignition and EVO timings. It is considered that the changes in CO concentration with respect to EVO timings result from the dilution of residual gas, mainly due to the backward flow during valve overlap period. These also indicate the effects of ignition timings are relatively weak compared to the effects of EVO timings.

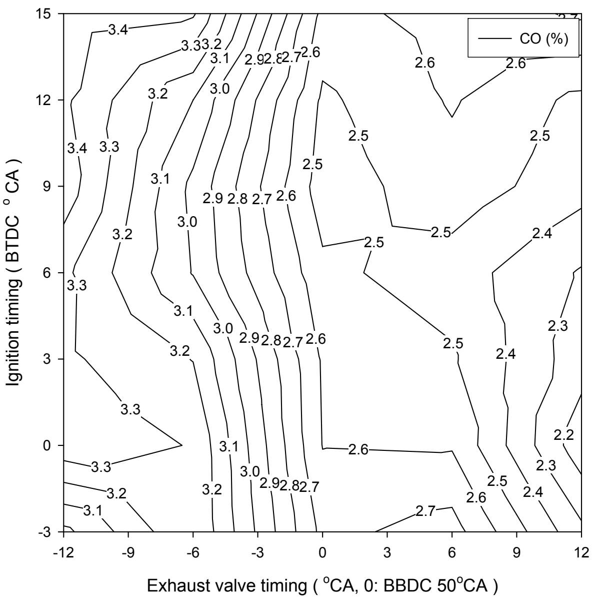

Fig. 8 Distribution of CO concentration with respect to ignition and EVO timings

Fig. 9 shows NOx concentrations with respect to the test conditions. It is clear that the concentrations of NOx decrease when the EVO is retarded. In SI engines, NOx emission depends on temperature of burned gas. When the EVO is retarded, residual gas fraction increases due to the increase of valve overlap period. Such residual gas is sometimes referred as internal EGR. Decreases of flame speed and increases of average specific heat are the representative effects of EGR. Consequently, the NOx concentrations depend on the EVO changes, due to the changes in residual gas fraction. It also supports that the COV variations of Fig. 3 depend mainly on the changes of residual gas and retarded EVO causes increase of residual gas in the cylinder on Fig. 7. In the Fig. 9, ignition timing is not a dominant factor that affects NOx concentration, but retarded ignition timings slightly increase NOx emissions, especially when the EVO timing is advanced. It shows that the retarded ignition timing increases the temperature in the cylinder under idle operation. At medium or high speed operations, retarded ignition from MBT timing causes decrease of maximum flame temperature and cylinder pressure, due to the expansion stroke of a piston. However, mean piston speed of idle operations is lower and flame stays longer in the expansion stroke, when ignition timings are retarded. Our previous study showed that retarded ignition timings increase exhaust gas temperature, due to the late appearance of maximum rate of heat release [8].

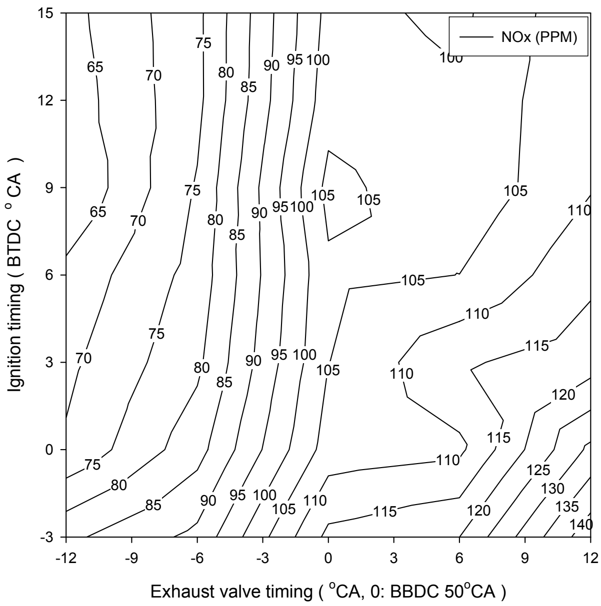

Fig. 9 Distribution of NOx concentration with respect to ignition and EVO timings

From these results, it is clear that the changes in EVO timings cause residual gas in the cylinder, and there are two opposite effects on exhaust gas composition and the stability of combustion. Advanced EVO is effective to reduce COV_{imep} and CO, but it also increases NOx emission. The effects are similar with the effects of EGR. Especially, these factors may interact more strongly in idle operations. Therefore, the controls should be much more precise in idle and cold-start operations. In Fig. 3, faster increase of COV_{imep} is observed when EVO is retarded from +3~+6° CA. At the same time, CO concentrations also show fast increase from the same EVO timings. Therefore, advanced EVO about 4~5° CA, which is BBDC 45~46° CA is considered as an optimal EVO timing of the test engine in terms of stability and CO emission. NOx emissions should be compromised to achieve combustion stability, or additional strategies for effective reductions of NOx should be suggested, to meet these two goals at the same time.

Fig. 10 shows emission concentrations of THC, with respect to test conditions. On the contraries to CO and NOx emissions, HC emissions depend on changes in ignition timings. Generally, two major parameters that determine HC emissions are flame temperature and duration of combustion. Increased exhaust gas temperature due to the retarded ignition timing causes reduction of HC emission and burned HC leads to the increase of exhaust gas temperature. From the experiments, it is possible that retarded ignition timings are efficient for the reduction of HC, in addition to the increase of exhaust gas temperature. However, slight increase of COV_{imep} and NOx emissions are also observed. In the point of view of COV_{imep}, it is considered that the retarded ignition timing of near BTDC 3° CA will compromise HC and COV_{imep}.

After all, the retarded ignition and advanced EVO is beneficial to increase exhaust gas temperature and to improve combustion stability. These idle control strategies can help reductions of exhaust emission. Additional strategies for effective reductions of NOx should be suggested, such as control of the amount of fuel. Unexpected problems on transient operating regions should be considered in order to apply to these control strategies.

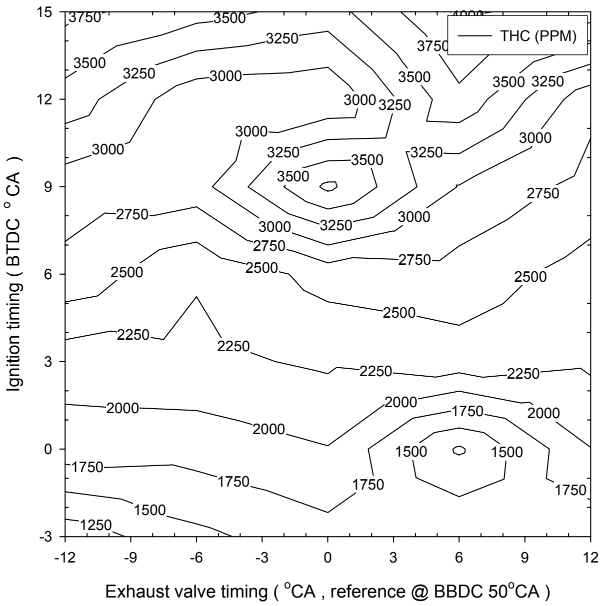

Fig. 10 Distribution of THC concentration with respect to ignition and EVO timings

5. CONCLUSIONS

In this study, the effects of EVO and ignition timings on idle operation are investigated through engine bench tests. Variations of COV_{imep} are estimated through the cylinder pressure analysis. Concentrations of CO, HC and NOx emissions are also investigated and analyzed. The numerical analysis supports reasons of these variations with respect to EVO. Followings are the conclusions of the study.

1. The stability of combustions depends on the changes in EVO, and an advanced EVO helps improvement of combustion stability. Residual gas fraction due to changes in valve overlap period may be the one of major reasons. When the EVO becomes excessively retarded or advanced, ignition timing slightly influences the stability.
2. CO and NOx emissions are sensitively varied with the changes in EVO timings. Retarded EVO results in the increase of CO and decrease of NOx. Dilution of fresh air with residual gas affects CO concentrations. An internal EGR effect of residual gas controls NOx concentrations.
3. Changes in ignition timings are the main parameter of hydrocarbon emissions and retarded ignition timings lead to decrease of HC concentration. It is considered that the changes of heat release characteristics can determine the cylinder temperature as well as duration of combustion process.
4. The retarded ignition and advanced EVO will be helpful to increase exhaust gas temperature and to improve combustion stability. These idle control strategies can help reductions of exhaust emissions Controls of NOx emission and unexpected problems on transient operating regions should be considered in order to apply to the control strategies.

ACKNOWLEDGEMENTS

This work is part of the project 'Development of Partial Zero Emission Technology for Future Vehicle' and we are grateful for its financial support.

REFERENCES

1. C. Summers, et al., "Use of Light-Off Catalysts to Meet the California LEV/ULEV Standards," *Society of Automotive Engineering*, 930386, 1993.
2. Yong-Seok Cho, et al., "Flow Distribution in a Close-Coupled Catalytic Converter," *Society of Automotive Engineering,* 982552, 1998.
3. S. Russ, G. Lavoie and W. Dai, "SI Engine Opeation with Retarded Ignition: Part 1 – Cyclic Variations," *Society of Automotive Engineering*, 1999-02-3506, 1999.
4. S. Russ, G. Lavoie and W. Dai, "SI Engine Operation with Retarded Ignition: Part 2 – Emissions and Oxidation," *Society of Automotive Engineering*, 1999-02-3507, 1999.
5. Charles E. Roberts and Rudolf H. Stanglmaier, "Investigation of Intake Timing Effects on the Cold Start Behavior of a Spark Ignition Engine," *Society of Automotive Engineering*, 1999-02-3622, 1999.
6. John B. Heywood, "Internal Combustion Engine Fundamentals," McGraw-Hill, 1988.
7. "FLUENT user's manual v. 6.1.," FLUENT research Corporation, 2003
8. Duk-Sang Kim, et al., "Variation of Exhaust Gas Temperature with the Change of Spark timing and Exhaust Valve Timing During Cold Start Operation of an SI Engine," Transactions of the Korean Society of Mechanical Engineers B, Vol. 25, No. 3, pp. 384-389, 2005.